Magnetization switching in alternating width nanowire arrays

S. Goolaup and A. O. Adeyeye*
Information Storage Materials Laboratory, Department of Electrical and Computer Engineering, National University of Singapore, 4 Engineering Drive 3, 117576, Singapore

N. Singh
Institute of Microelectronics, 11 Science Park Road, Singapore Science Park II, 117685, Singapore

G. Gubbiotti
CNISM, Dipartimento di Fisica, Università di Perugia, Via A. Pascoli, I-06123 Perugia, Italy
(Received 8 December 2006; revised manuscript received 14 February 2007; published 30 April 2007)

A systematic investigation of the magnetization reversal mechanism in arrays of $Ni_{80}Fe_{20}$ nanowires with alternating width is presented. The structures were fabricated using deep ultraviolet lithography followed by lift-off technique at 248 nm exposure wavelength. We have mapped the magnetization reversal processes and observed that the switching mechanism is very sensitive to the thickness to width ratio of the nanowires. For wire thickness, $t \leqslant 40$ nm, spin rotation dominates the reversal process. For $t > 40$ nm, however, the reversal process is mediated by the curling mode of reversal. The dipolar field is strongly influenced by the nanowire of larger width in the alternating width array. Our results were compared with homogeneous width nanowire array of similar thicknesses and marked differences were observed.

DOI: 10.1103/PhysRevB.75.144430 PACS number(s): 75.75.+a, 75.60.Jk

I. INTRODUCTION

Patterned arrays of highly ordered nanomagnets have attracted a lot of attention as they are ideally suited for testing micromagnetic models and because of their application in nonvolatile magnetic data storage.[1–3] The reduced lateral dimensions of the materials have drastic effects on the fundamental magnetic properties such as the magnetization reversal mechanisms. There is growing interest in magnetic nanowire (NW) arrays both from a fundamental perspective and because of their potential applications in magnetoelectronic devices. A lot of research has focused on understanding both the static[4–7] and dynamic properties[8–11] of homogeneous width ferromagnetic nanowire arrays. It has been observed that the magnetic properties of NWs are strongly dependent on the lateral size due to the spatially varying demagnetizing field.[4] The reversal process in ferromagnetic wires changes from domain wall motion to spin rotation as the wire width is reduced. Recently, we have shown a transition from spin rotation to curling mode of magnetization reversal in homogeneous $Ni_{80}Fe_{20}$ NW arrays as the $Ni_{80}Fe_{20}$ film thickness is increased.[7] It has also been shown that the interwire spacing in NW arrays greatly influences the magnetic properties. The magnetostatic coupling in wire arrays may give rise to a step-wise demagnetization curve.[12–14] The coercivity of NW arrays was found to be influenced, as the edge-to-edge spacing of the wire becomes comparable to the wire width.[15]

While most of the research has focused on vertically stacked multilayer NWs with a view for application in miniaturized advanced read head sensor and nonvolatile magnetic random access memories, few works have exploited the lateral engineering of wire arrays. Adeyeye *et al.*[16] investigated the magnetic properties of lateral $Co/Ni_{80}Fe_{20}$ micron sized wires. A state of antiparallel alignment of the magnetization was observed, due to the differential coercivity of the Co and $Ni_{80}Fe_{20}$ wires. Variable width ferromagnetic wire arrays were also investigated. The coercivity of the wire arrays can be engineered by alternating wires of different width in an array.[17]

In this work, we report on the systematic investigation of the magnetization switching in laterally engineered $Ni_{80}Fe_{20}$ NW arrays. It has been shown before that the switching field of wire arrays of a fixed film thickness is highly sensitive to the wire width and it increases as the wire width is reduced.[4] By exploiting the width dependence of the coercivity, we have fabricated alternating width NW arrays with unique magnetic properties. The structure consists of two differential width $Ni_{80}Fe_{20}$ NWs alternated in an array. We observed that the magnetization reversal process is sensitive to the wire thickness to width ratio. The dipolar interaction between the individual wires in the alternating width NW array was probed using minor loop measurements. We also observed that the interaction field is strongly dependent on the individual wire width constituting the array.

II. EXPERIMENTAL DETAILS

Two types of $Ni_{80}Fe_{20}$ NW arrays of alternating width, consisting of two sets of NWs of width $w_1 = 330$ nm, $w_2 = 530$ m ($\Delta w = 200$ nm) and $w_1 = 330$ nm, $w_2 = 900$ nm ($\Delta w = 570$ nm) alternated in an array, were fabricated on silicon substrate using deep ultraviolet lithography. A control experiment (reference NW array) consisting of homogeneous NW arrays of width $w = 330$ nm was also patterned using the same technique. For all the geometries, the length of all the NW arrays was maintained at 4 mm, while the patterned area is 16 mm^2. The large patterned area ensures that the magnetic properties of the NWs can be characterized using vibrating sample magnetometer. In order to ensure that the NWs are magnetostatically coupled, the edge-to-edge spac-

ing for all the NW arrays patterned was maintained at 70 nm. Polycrystalline $Ni_{80}Fe_{20}$ of thickness (t) in the range from 20 nm to 100 nm was deposited by dc magnetron sputtering at room temperature. The base pressure of the chamber was better than 2×10^{-8} Torr before deposition. Lift-off was conducted in resist thinner OK73 and isopropyl alcohol (IPA). Ultrasonic bath was used to assist the lift-off of the magnetic layer. Completion of the lift-off process was determined by the color contrast of the patterned $Ni_{80}Fe_{20}$ area and confirmed by inspection under a scanning electron microscope (SEM). The SEM images of the alternating and homogeneous width NW arrays are shown in Fig. 1. The large area view shows well-defined wires with uniform wire spacing and good edge definition. The insets display a magnified image of the wire arrays. Details of the fabrication process are described in Ref. 18.

III. RESULTS AND DISCUSSION

A. Magnetic properties of alternating width nanowires

In Fig. 2(a) we present the representative M-H loops for 70 nm thick $Ni_{80}Fe_{20}$ NW arrays for fields applied along the long (easy) axis of the wires. Both alternating width NW arrays display a totally different M-H behavior as compared to the homogeneous width NW array. The homogeneous NW array with $w_1=w_2=330$ nm, as expected, displays an almost rectangular M-H loop with a coercivity of 170 Oe.

For alternating width NW array with $\Delta w=200$ nm, however, we observed a double step hysteresis loop. As the applied field is reduced from positive saturation, a sharp drop in magnetization within the field range of -30 Oe to -100 Oe was observed. Beyond this field, a gradual decrease in magnetization is seen until an external field of -190 Oe. This is followed by an abrupt drop in magnetization leading to negative saturation. A similar trend was observed for alternating width NWs with $\Delta w=570$ nm, although the switching fields are shifted to lower external fields due to the contribution from the larger width wire. As can be seen from Fig. 2(a), the first drop in magnetization for alternating width NW with $\Delta w=570$ nm occurs within the field range of -13 Oe to -75 Oe, followed by a quasistable plateau until an external field of -145 Oe. The magnetization then decreases monotonically until negative saturation is achieved at an external field of -265 Oe.

We observed that following the first switching in $\Delta w=200$ nm, a drop of 65% of the total magnetization is seen, whereas $\Delta w=570$ nm displays a much larger drop of 78%, as seen in Fig. 2(a). For a fixed film thickness, the drop in the magnetization will be proportional to the individual wire width of the alternating NW array. The drop in magnetization following the reversal of the larger width wire, w_2, in the array will be proportional to the volume fraction (w_2/w_1+w_2). For our geometry we expect a drop of 62% for $\Delta w=200$ nm and 73% for $\Delta w=570$ nm, which is in good agreement with the experimental result.

In Fig. 2(b), we plotted the differentiated half M-H loop, for fields applied from positive to negative saturation, for the 70 nm $Ni_{80}Fe_{20}$ thick NW arrays. For the homogeneous wire, we observed a broad base peak, with the maximum at an external field of -175 Oe. This value is consistent with the coercivity obtained from the M-H loop. As expected for $\Delta w=200$ nm and 570 nm, two peaks corresponding to the switching of the two sets of wires, w_1 and w_2, comprising the array, are seen in Fig. 2(b). The first peak corresponds to the

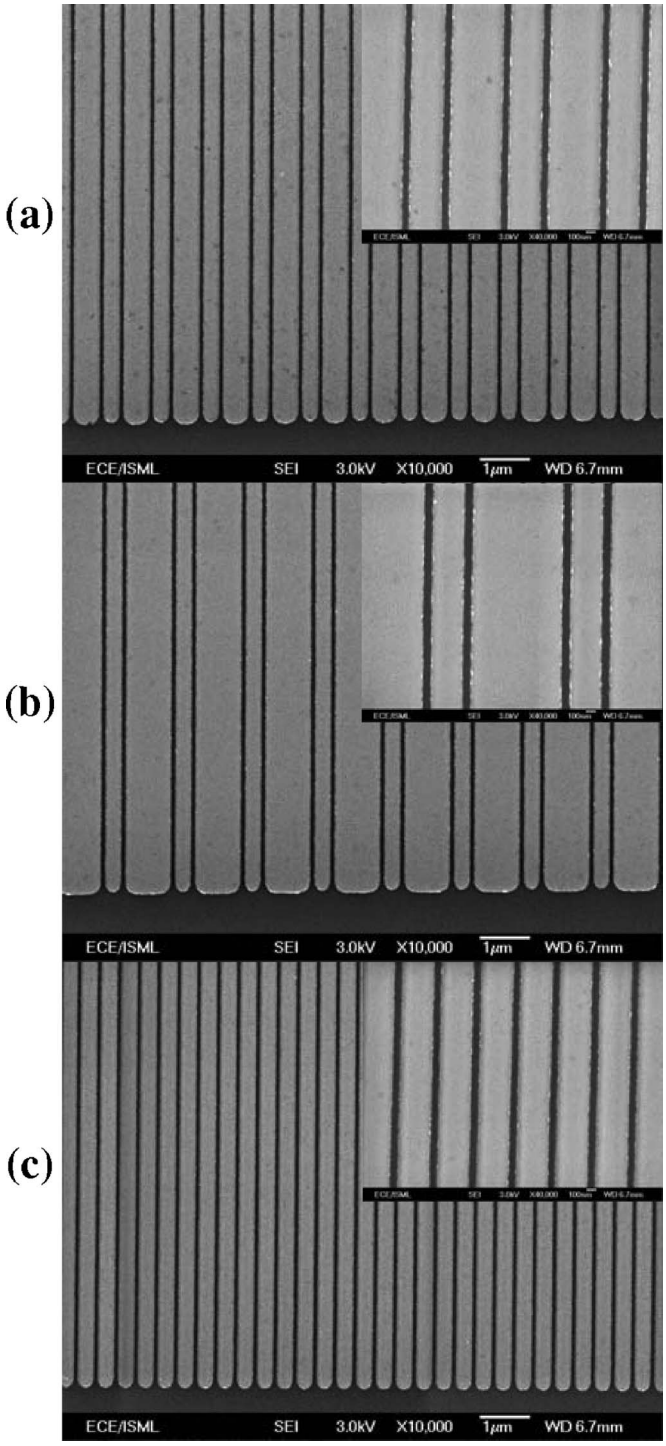

FIG. 1. Scanning electron micrograph of 40 nm $Ni_{80}Fe_{20}$ thick; alternating nanowire arrays with (a) $\Delta w=200$ nm consisting of wires $w_1=330$ nm; $w_2=530$ nm, (b) $\Delta w=570$ nm consisting of wires $w_1=330$ nm; $w_2=900$ nm, (c) homogeneous width nanowire array with width =330 nm. The edge-to-edge spacing for all the nanowire arrays is maintained at 70 nm.

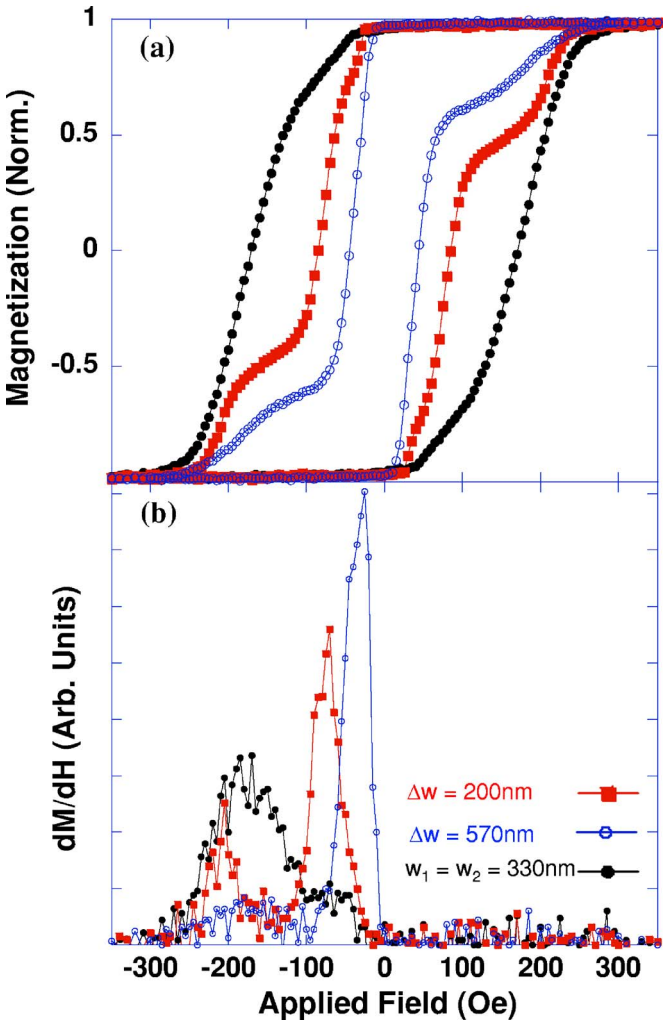

FIG. 2. (Color online) (a) Magnetic hysteresis loops for 70 nm thick $Ni_{80}Fe_{20}$ film for fields applied along the long axis (θ=0°); (b) differentiated *M-H* loops, for the alternating nanowire arrays, Δw=200 nm, and Δw=570 nm and reference nanowire arrays.

low field switching of the larger width wire w_2, while the second peak corresponds to the high field switching of the smaller wire width w_1. For Δw=200 nm, the switching of w_1 and w_2 occurs at an external field of −205 Oe and −70 Oe, respectively. For Δw=570 nm, however, the switching of w_1 and w_2 are at −190 Oe and −25 Oe, respectively. As w_1 is the same for both alternating width NW arrays, the difference in the switching fields may be attributed to the effects of the magnetostatic coupling, due to the small interwire spacing s=70 nm, between the wires in the array which greatly influences the reversal process.

Based on the differentiated half *M-H* loop, Fig. 2(b), the clear and distinct differences between the two peaks in the curve imply that a region of antiparallel alignment in the magnetization of neighboring wires in the array exists. In Fig. 3, a schematic representation of the possible magnetic states in the 70 nm thick $Ni_{80}Fe_{20}$ alternating width NW arrays as the field is swept from positive to negative saturation is presented. At positive saturation, the magnetization of all the wires are aligned along the field direction as seen in Fig. 3(a). At the occurrence of the first peak in the dM/dH, in

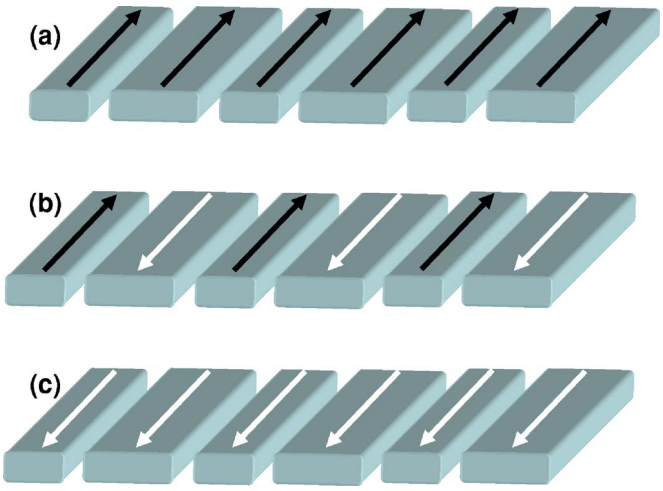

FIG. 3. (Color online) Representative *M-H* loops for the alternating nanowire arrays, Δw=200 nm and Δw=570 nm, and reference nanowire arrays as a function of the $Ni_{80}Fe_{20}$ film thickness.

Fig. 2(b), the larger w_2 wire in the alternating width NW array switches towards the field direction, as shown in Fig. 3(b). Further decrease of the field leads to the switching of the smaller wire, w_1, constituting the alternating width NW array. This corresponds to the second peak observed in Fig. 2(b), as shown in the schematic in Fig. 3(c).

B. Effect of wire thickness

In order to understand the effect of other geometrical parameters such as the film thickness on the magnetic properties of the alternating width NWs, we carried out a systematic thickness dependent study. The $Ni_{80}Fe_{20}$ film thickness was varied from 20 nm to 100 nm, while all other geometric parameters of the wire arrays were kept fixed. In Fig. 4, we present the representative *M-H* loops for fields applied along the long (easy) axis of the NW arrays, as a function of the

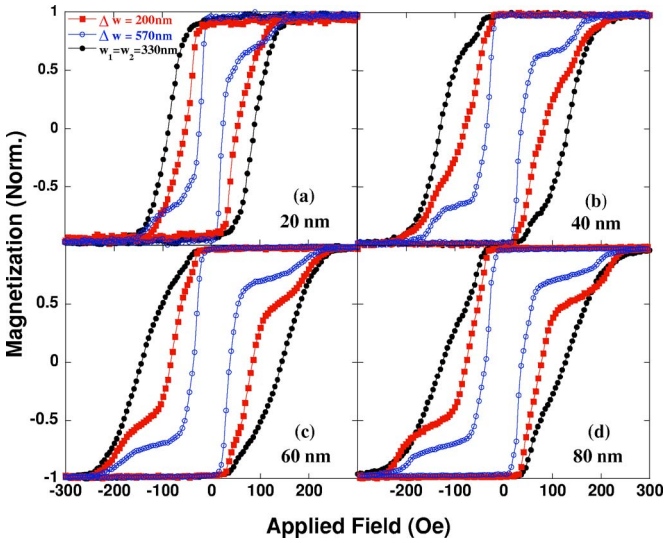

FIG. 4. (Color online) Schematic representation of the different states of the 70 nm thick $Ni_{80}Fe_{20}$ alternating width nanowires.

$Ni_{80}Fe_{20}$ film thickness. For $t=20$ nm, the homogeneous width NW array displays an almost rectangular *M-H* loop with a coercivity of 88 Oe, as shown in Fig. 4(a). For the alternating width NW arrays with $\Delta w=200$ nm, a sharp drop in magnetization at an external field of −20 Oe, followed by a slight tilt in the hysteresis loop. As the switching of the w_1 and w_2 wires are comparable for $\Delta w=200$ nm, switching field distribution may lead to a broadening of the switching field for each set of wires, resulting in the observed tilt in the *M-H* loop. For $\Delta w=570$ nm, however, we observed that the reversal process is mediated by a clear two-step switching, as shown in Fig. 4(a). As the field is reduced from positive saturation, an abrupt drop in magnetization occurs at an external field of −15 Oe, due to the reversal of w_2 in the alternating width NW array. As the field is further reduced, a gradual decrease in magnetization is seen in the field range of −36 Oe to −100 Oe. Further decrease in the external field leads to a sharp switching, resulting in negative saturation.

In Fig. 4(b), we observed that for $t=40$ nm, there is an increase in the coercivity for all the NW arrays. The coercivity of the homogeneous NW increases to 130 Oe. Interestingly, for $\Delta w=200$ nm, we observed a transition towards a double-step reversal, with a sharp drop in magnetization occurring at an external field of −25 Oe. The NW arrays with $\Delta w=570$ nm on the other hand display a more distinct two step reversal with a quasistable plateau within the field range of −65 Oe to −120 Oe.

When the $Ni_{80}Fe_{20}$ film thickness is increased to 60 nm, we observe a further increase in coercivity, to 145 Oe, of the homogeneous NW array, accompanied by a slight shearing of the *M-H* loop. The alternating width NW array with $\Delta w=200$ nm exhibits a distinct two-step reversal. For $\Delta w=570$ nm, the field range over which the stable region extends from −80 Oe to −160 Oe.

Interestingly, when the film thickness is increased to 80 nm, a noticeable decrease of the coercive field for all the NW arrays was observed. The coercivity of the homogeneous NW array decreases to 125 Oe, and with the shearing of the *M-H* loop being more pronounced. We have earlier reported a similar thickness dependent coercive behavior for homogeneous width $Ni_{80}Fe_{20}$ NW array. This was attributed to a change in the magnetization reversal mechanism in the NWs.[7] For $\Delta w=200$ nm, the magnetization loop displays a small region of antiparallel alignment, with a quasistable plateau within the field range of −110 Oe to −190 Oe. For $\Delta w=570$ nm, however, the plateau-like region is in the range of −75 Oe to −185 Oe.

The evolution of the *M-H* curve as a function of the $Ni_{80}Fe_{20}$ film thickness may be attributed to the spatially varying demagnetizing field along the width of the alternating NW array. When the $Ni_{80}Fe_{20}$ film thickness is increased, the thickness to width ratio of w_1 and w_2, constituting the alternating nanowire array, will change at different rates. Thus, as t is increased, the switching of the two sets of NWs, w_1 and w_2, constituting the array becomes more distinct, resulting in double-step reversal.

For all the thickness range investigated, we estimated the switching field distribution (SFD) by differentiating one branch of the hysteresis loop. The peaks represent the switching of the respective wires, w_1 and w_2, whereas the base reflect the SFD. The broader the base, the larger is the SFD.[19] We observed that the homogeneous NW array and alternating width NW with $\Delta w=200$ nm, exhibit much larger SFD, as compared to $\Delta w=570$ nm, as seen in Fig. 4. The SFD during the reversal of nanostructures is attributed to the process variation and the dipolar coupling between the elements. From the SEM image, the shape homogeneity of the NW array is confirmed, thus we attribute the broadening of the slope in the *M-H* curve to the dipolar coupling between the NWs in the array. For the larger width wires, we expect the formation of edge domains at the end of the wires as the field is relaxed along the wire axis. The edge domains inhibit the accumulation of magnetic charges at the wire end, thus reducing the effective coupling field between alternate wires. This is evidenced by the abrupt drop in magnetic moment for $\Delta w=570$ nm, for all thicknesses investigated.

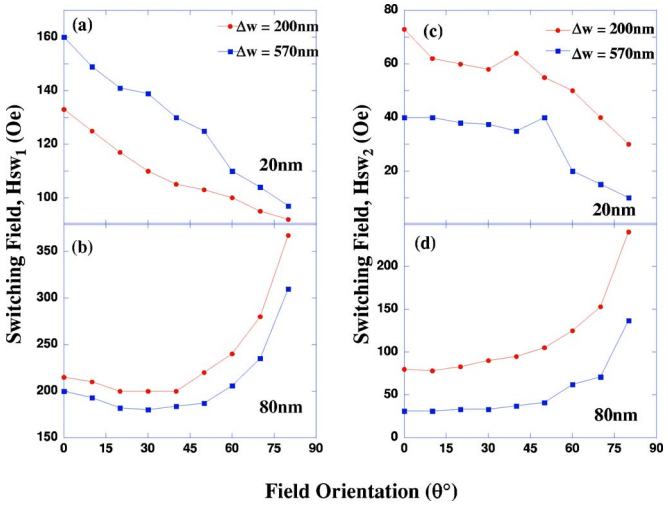

FIG. 5. (Color online) Representative switching field as a function of the field orientation with respect to the wire axis of the alternating width nanowire arrays with $\Delta w=200$ nm and $\Delta w=570$ nm, for $Ni_{80}Fe_{20}$ film thickness 20 nm and 80 nm.

C. Magnetization reversal mechanisms

To gain an insight into the magnetization reversal process of the alternating width NWs, we carried out a systematic field orientation dependent study of the *M-H* loops. The angular dependence of the switching field has been shown to provide information about the magnetization reversal mode in NWs. Angular dependent measurements were carried out by varying the orientation of the applied field relative to the NW easy axis from 0° to 80° in steps of 10°. We have extracted the switching field of the wires w_1 and w_2 comprising the alternating width NW array. Shown in Fig. 5 are the representative angular variations of the switching field of the two NWs, w_1 (Hsw_1) and w_2 (Hsw_2), constituting the alternating width NW arrays for $\Delta w=200$ nm and $\Delta w=570$ nm. In our structures for fields applied along the long axis of the wires, we expect the reversal process at the end of the wires to be mediated by the formation of end domains. The angular variation of the switching field gives an insight into the reversal process of the central region of the wires.

In Figs. 5(a) and 5(b) we present the switching field variation for w_1 wires for both alternating width NWs, $\Delta w = 200$ nm and $\Delta w = 570$ nm. When $t = 20$ nm, we observed that the switching field variation of w_1 for both $\Delta w = 200$ nm and $\Delta w = 570$ nm decreases monotonically as the field orientation is increased from $\theta = 0°$, as seen in Fig. 5(a). The minimum switching field occurs when the applied field is along $\theta = 80°$. As we have previously reported,[7] this angular variation of switching field is consistent with the reversal process by spin rotation.

For $t = 80$ nm, the field orientation dependence of the switching field for w_1 wires constituting the alternating width NWs is shown in Fig. 5(b). As the field orientation θ is increased from 0°, a slight decrease in the switching field is observed. Within the field orientation, $20° \leqslant \theta \leqslant 40°$, an almost constant Hsw_1 is obtained. For $\theta > 40°$, a sharp increase in the switching field is observed. The maximum switching field occurs when the applied field orientation is along $\theta = 80°$. This angular switching field variation is characteristic of the curling mode of reversal. For an infinite cylinder, the angular variation of Hsw in the curling mode of reversal is given by[20]

$$H_{sw} = \frac{M_s}{2} \frac{a(1+a)}{\sqrt{a^2 + (1+2a)\cos^2\theta}},$$

where $a = -1.08(d_0/d)^2$. The exchange length $d_0 = 2\sqrt{A}/M_s$ and A is the exchange constant. In the curling regime, minimum field occurs for fields applied along the long axis of the wire. The switching field increases as a function of the field orientation, with the maximum switching field occurring for fields applied along $\theta = 90°$.

The angular variation of the switching field for the larger width wire, w_2, comprising the alternating width NWs when $t = 20$ nm is shown in Fig. 5(c). For $\Delta w = 200$ nm, we observed a slight decrease in the switching field as the field orientation is increased from $\theta = 0°$ to 10°. This is followed by a plateaulike region with the field orientation range of $10° \leqslant \theta \leqslant 40°$. When $\theta = 50°$, a slight increase in the switching field is seen, resulting in a local maxima. As the field orientation is further increased, $\theta > 50°$, the switching field decreases, reaching a minimum when $\theta = 80°$. For $\Delta w = 570$ nm, we observed a similar switching field trend with the peak occurring along $\theta = 50°$. The switching field variation for both sets of w_2 wires, comprising the alternating width NW in $\Delta w = 200$ nm and $\Delta w = 570$ nm, implies that the reversal process is dominated by spin rotation.

In Fig. 5(d), we present the angular variation of the switching field for w_2 wires, of the alternating width NW arrays $\Delta w = 200$ nm and $\Delta w = 570$ nm, for $t = 80$ nm. We observed that the switching field, for both set of w_2 wires, increases as a function of the orientation of applied field, similar to the w_1 NW as seen in Fig. 5(b). This angular variation of the switching field is also consistent with the curling mode of rotation.[20–22]

D. Minor loop measurements

To further understand the magnetization reversal process we carried out minor loop measurements. The minor loop has been used previously to quantify the interaction field and coercivity of pseudospin valve (PSV) elements.[19] The minor loop offset represents the interaction field, whereas the minor loop width is equal to 2 times the coercivity of the soft layer in the PSV. We have used the minor loop measurement to obtain the field $H_{w1\text{-}w2}$ exerted by the smaller width wire, w_1, on the larger width wire, w_2, and to determine the effective coercivity of the larger width wire, $H_{c\text{-}w2}$, in the alternating NW arrays. We carried out a systematic minor loop measurement for both sets of alternating NW arrays. The NWs were first saturated with an applied field of 300 Oe along the wire axis. The field was then reduced to a predetermined reversing field (H_m), and increased to positive saturation again. Shown in Fig. 6(a) are the representative minor loops and corresponding full loop for the 80 nm thick arrays of $Ni_{80}Fe_{20}$ alternating width NWs for $\Delta w = 200$ nm. We observed that as H_m is reduced to −40 Oe, there is a broadening in the saturation region of the minor loop. This is due to the incomplete reversal of all the w_2 NWs for $\Delta w = 200$ nm. Within the field range, $-90 \text{ Oe} \leqslant H_m \leqslant -120$ Oe, we observed that the saturation field of the minor loop coincides, implying that most of the w_2 wires have switched, but the field is not strong enough

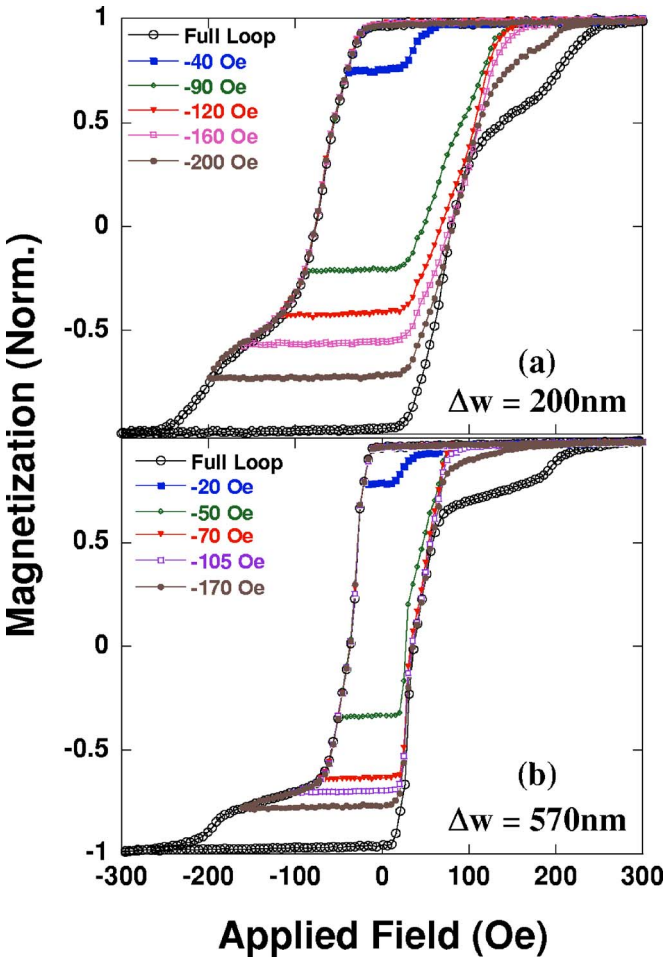

FIG. 6. (Color online) Representative M-H loops and minor loops for 80 nm $Ni_{80}Fe_{20}$ alternating nanowire arrays with (a) $\Delta w = 200$ nm, (b) $\Delta w = 570$ nm, as a function of the reverse field, H_m.

TABLE I. Interaction fields ($H_{w1\text{-}w2}$) and effective coercivity ($H_{c\text{-}w2}$) obtained from minor loops.

t (nm)	$H_{w1\text{-}w2}$ $(\text{Oe})_{200\ \text{nm}}$	$H_{c\text{-}w2}$ $(\text{Oe})_{200\ \text{nm}}$	$H_{w1\text{-}w2}$ $(\text{Oe})_{570\ \text{nm}}$	$H_{c\text{-}w2}$ $(\text{Oe})_{570\ \text{nm}}$
40	6	67	2.5	32
60	8	78	3.5	39.5
70	11	84	5	43
80	13	79	5.5	35.5
100	8	53	4	35

to switch the w_1 wires. As H_m is further reduced, $H_m \leqslant 120$ Oe, the minor loop again displays a broadening in the saturation region, indicating the onset of reversal of the w_1.

The broadening in the saturation of the minor loop, as the field is increased towards positive saturation, is due to the incomplete switching of the w_1 wires in the array. Similarly, for $\Delta w = 570$ nm, we observed a similar minor loop behavior as H_m is increased towards negative saturation, as shown in Fig. 6(b). For $-70\ \text{Oe} \leqslant H_m \leqslant -50$ Oe, the saturation field of the minor loop for $\Delta w = 570$ nm coincides, indicating an almost complete reversal of the NW w_2 within this field range. As H_m is further decreased beyond -70 Oe, the broadening in the saturation indicates the reversal of the w_1 wires in $\Delta w = 570$ nm. This confirms that the reversal process in the array of alternating width NWs is mediated by the switching of the larger width wire w_2 followed by the smaller width wire w_1.

We have extracted the effective coercivity of w_2, $H_{c\text{-}w2}$, and field exerted by the wire w_1 on w_2, $H_{w1\text{-}w2}$, for both sets of alternating NW arrays for different $Ni_{80}Fe_{20}$ film thicknesses, as shown in Table I. Both the interaction field and effective coercivity for $\Delta w = 200$ nm is about 2 times the corresponding value for $\Delta w = 570$ nm, for all the thicknesses investigated. As discussed earlier, this is expected due to the larger difference in NW width. Interestingly, we observed that for both sets of alternating NW arrays, the effective coercivity, $H_{c\text{-}w2}$, of w_2 decreases for $t \geqslant 80$ nm. For $t = 100$ nm, we expect the reversal process to be wholly dominated by the curling mode of reversal. The decrease in the effective coercivity of w_2 may be due to a change in the reversal mechanisms of both w_1 and w_2 wires constituting the array. The interaction field increases with $Ni_{80}Fe_{20}$ film thickness, for $t \leqslant 80$ nm. When $t = 100$ nm, we observed that both sets of alternating width NW arrays display a decrease in the interaction field. This may be due to the significant decrease in the effective coercive field of w_2. As the curling mode of reversal minimizes the magnetostatic energy of the individual wires in the array, a drop in the dipolar field between the wires is expected.

IV. CONCLUSION

In summary, we have carried out a systematic investigation of the magnetic properties of alternating width NW arrays fabricated using deep ultraviolet lithography. The magnetization reversal process of the laterally engineered NWs is markedly sensitive to the wire thickness to width ratio. We observed that the magnetization reversal process is strongly influenced by both the wire width and $Ni_{80}Fe_{20}$ film thickness. The dipolar coupling is strongly dependent on the larger width wire constituting the alternating width array.

ACKNOWLEDGMENTS

This work was supported by National University of Singapore (NUS) under Grant No. R-263-000-283-112. One of the authors (S.G.) would like to thank NUS for his research scholarship.

*Corresponding author; Electronic address: eleaao@nus.edu.sg

[1] M. Hehn, K. Ounadjela, J. P. Bucher, F. Rousseaux, D. Decanini, B. Bartenlian, and C. Chappert, Science **272**, 1782 (1996).
[2] G. A. Prinz, Science **282**, 1660 (1998).
[3] R. L. White, R. M. H. Newt, and R. F. W. Pease, IEEE Trans. Magn. **33**, 990 (1997).
[4] A. O. Adeyeye, J. A. C. Bland, C. Daboo, Jaeyong Lee, U. Ebels, and H. Ahmed, J. Appl. Phys. **79**, 6120 (1996).
[5] W. Wernsdorfer, B. Doudin, D. Mailly, K. Hasselbach, A. Benoit, J. Meier, J. Ph. Ansermet, and B. Barbara, Phys. Rev. Lett. **77**, 1873 (1996).
[6] J. E. Wegrowe, D. Kelly, A. Franck, S. E. Gilbert, and J.-Ph. Ansermet, Phys. Rev. Lett. **82**, 3681 (1999).
[7] S. Goolaup, N. Singh, A. O. Adeyeye, V. Ng, and M. B. A. Jalil, Eur. Phys. J. B **44**, 259 (2005).
[8] G. Gubbiotti, S. Tacchi, G. Carlotti, P. Vavassori, N. Singh, S. Goolaup, A. O. Adeyeye, A. Stashkevich, and M. Kostylev, Phys. Rev. B **72**, 224413 (2005).
[9] S. M. Chérif, Y. Roussigné, C. Dugautier, and P. Moch, J. Magn. Magn. Mater. **222**, 337 (2000).
[10] G. Gubbiotti, M. Kostyleva, N. Sergeevaa, M. Conti, G. Carlotti, T. Ono, A. N. Slavin, and A. Stashkevich, Phys. Rev. B **70**, 224422 (2004).
[11] G. Gubbiotti, G. Carlotti, T. Ono, and Y. Roussigne, J. Appl. Phys. **100**, 023906 (2006).
[12] L. C. Sampaio, E. H. C. P. Sinnecker, G. R. C. Cernicchiaro, M. Knobel, M. Vázquez, and J. Velázquez, Phys. Rev. B **61**, 8976 (2000).
[13] J. Velázquez, K. R. Pirota, and M. Vázquez, IEEE Trans. Magn. **39**, 3049 (2003).
[14] A. Chizhik, A. Zhukov, J. M. Blanco, R. Szymczak, and J. Gonzalez, J. Magn. Magn. Mater. **249**, 99 (2002).
[15] A. O. Adeyeye, J. A. C. Bland, C. Daboo, and D. G. Hasko, Phys. Rev. B **56**, 3265 (1997).
[16] A. O. Adeyeye, M. K. Husain, and V. Ng, J. Magn. Magn. Mater. **248**, 355 (2002).
[17] A. O. Adeyeye, J. A. C. Bland, and C. Daboo, J. Magn. Magn. Mater. **188**, L1 (1998).

[18] N. Singh, S. Goolaup, and A. O. Adeyeye, Nanotechnology **15**, 1539 (2004).
[19] F. J. Castano, Y. Hao, M. Hwang, C. A. Ross, B. Vogeli, Henry I. Smith, and S. Haratani, Appl. Phys. Lett. **79**, 1504 (2001).
[20] W. F. Brown, Phys. Rev. **105**, 1479 (1957); H. Frei, S. Shtrikman, and D. Treves, *ibid.* **106**, 446 (1957); S. Shtrikman and D. Treves, J. Phys. (Paris), Colloq. **20**, 286 (1959).
[21] A. Aharoni and S. Shtrikman, Phys. Rev. **109**, 1522 (1958).
[22] Y. Ishii, J. Appl. Phys. **70**, 3765 (1991).